ARTICLE

Development of Flexible LEO-Resistant PI Films for Space Applications Using a Self-Healing Mechanism by Surface-Directed Phase Separation of Block Copolymers

Hartmut R. Fischer,*,† Karin Tempelaars,† Aat Kerpershoek,† Theo Dingemans,‡ M. Iqbal,‡ Henk van Lonkhuyzen,§ Boris Iwanowsky,⊥ and Christopher Semprimoschnig⊥

TNO Science and Technology, P.O. Box 6235, 5600 HE Eindhoven, The Netherlands, Faculty of Aerospace Engineering, Delft University of Technology, Kluyverweg 1, 2629 HS Delft, The Netherlands, Dutch Space B.V., Mendelweg 30, 2333 CS Leiden, The Netherlands, and Materials Space Evaluation and Radiation Effects Section, ESA- ESTEC, P.O. BOX 299, Keplerlaan 1, NL 2200 AG Noordwijk, The Netherlands

ABSTRACT Polimide-*block*-polydimethylsiloxane (PI-*b*-PDMS) block copolymers have been synthesized from commercially available amino-terminated polysiloxanes with different molecular weights, for use as polymeric materials resistant to the low earth orbit (LEO) space environment. A structural optimization with respect to maximum environmental protection has been performed by varying the PDMS block length as well as the architecture of the block copolymers spanning from multiblock to triblock and star-shaped morphologies. The synthesized polymers and casted films show good mechanical and thermal performance. For block copolymers with a load of 2 % PDMS (in the case of the multiblock copolymers), a complete surface coverage of the PDMS has been found. It has been shown that the transfer of the surface enriched PDMS layer into a thin silica layer after atomic oxygen (AO) exposure results in a drastic decrease in AO erosion rate. The silica layer protects the underlying material from oxygen initiated erosion resulting in a drastic decrease of surface roughness. This phenomena is observable for loads as small as 6 wt % PDMS.

KEYWORDS: thermal control • PDMS-*b*-PI • atomic oxygen

INTRODUCTION

The present generation of spacecrafts, space stations, and satellites have a lifetime expectancy limited to 5−7 years, often as a result of environmentally induced degradation of the structural materials. Far from being just inert vacuum, low Earth orbit contains reactive atomic oxygen (AO), an increasing quantity of man made debris, natural micrometeoroids, ultraviolet radiation and large temperature extremes (1−3). Atomic oxygen is one of the main constituents in low Earth orbit (LEO; 200−700 km). The highly reactive oxygen atoms form as a result of photodissociation of diatomic oxygen molecules by solar photons having a wavelength of ≤243 nm. Spacecraft in LEO collide with this atomic oxygen at energies of 4.2−4.5 eV. As a result of the synergistic effect of all the mentioned factors, most polymers and polymer matrix composites degrade rapidly. For polymer materials targeted for space applications in LEO, such as flexible protective coatings for solar arrays, fiberglass structural elements and others, AO can play an essential role in their degradation. Erosion yields are typically on the order of 1×10^{-24} grams per incident AO atom (1, 3). Such conditions lead to a progressive surface degradation and limit the lifetime of today's orbiting spacecraft. Consequently, the integrity of structures would be lost before the end of the spacecraft's intended service lifetime. With the increasing importance of polymers in orbiting spacecraft, it has become imperative to determine how, and to what extent, the properties of polymers are affected. Knowing this, polymers suitable for LEO applications can be developed or selected. One option for protection of polymers is the application or introduction of thin (15−100 nm) coatings of transparent, LEO-resistant metal oxides on top of the polymeric matrix material (4). Although plasma-deposited SiO_x coatings perform well, they have not been utilized to date because on the one hand a minimum thickness of 15 nm is required for a reduction of the concentration of defects in the coating below a critical value, and a maximum of 100 nm has to be realized to retain certain flexibility without loss of integrity (appearance of cracks) (4). Tests on PVD coatings of Si, SiOx, SiN, and SiON show that these coatings provide good protection of underlying polymers. However their application imposes severe constraints. The thermal expansion coefficients of the coatings differ markedly from those of polymers, which can result in cracks developing during thermal cycling and penetration of AO through to the substrate. This can lead to undercutting phenomena and ultimately to mechanical

* Corresponding author. E-mail: hartmut.fischer@tno.nl.
Received for review March 15, 2010 and accepted July 5, 2010
† TNO Science and Technology.
‡ Delft University of Technology.
§ Dutch Space B.V.
⊥ ESA- ESTEC.
DOI: 10.1021/am100223v

Published on Web 08/06/2010

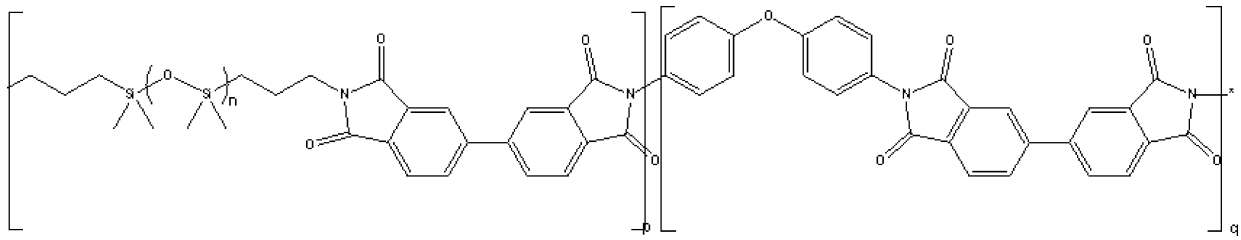

FIGURE 1. Principal structure of the synthesized PI-PDMS multiblock copolymers.

failure of the polymer when a sufficient number of undercut cavities connect (5, 6). Alternative technologies like the Photosil (7, 8) or the Implantox process (9−12) can also be used to protect surfaces. However, such treatments have to be applied on ground with substantial costs, and the solar absorbance of the material can be significantly altered.

A more ambitious option is to use siloxane composites, which are converted to SiO_2 by AO interaction (13−16). This surface layer is stable in vacuum and inhibits further oxidation. Siloxanes can therefore be exploited in the first instance as coatings but also alternatively as additivse to the polymeric matrix. A UV/ozone treatment of organic polymers having poly(dimethylsiloxane) (PDMS) additives in low concentrations (typically in the range of 0.1−2.0% by weight) produces oxidized layers of the surface-segregated PDMS (13), which protect the underlying material from further degradation (17).

More preferential is the use of covalently bound silicon compounds like siloxanes to provide a good adhesion between the convertible top layer and the structural polymeric material. The first records of the preparation of siloxane-modified polypyromellitimides dates back to 1966 (18) and of block copolymers of polyimide and siloxane to 1984 (19). In the latter case, the lower surface tension of the silicon component, which introduces microphase separation in covalently connected polymers, drives it toward the surface. On a thermodynamic basis, materials present in a mixture tend to orient themselves such that the resulting surface of the system has a minimized energy. If a molecule contains groups with different surface energies, molecular rearrangement or segregation of the lower surface energy component toward the surface is achieved. In a block copolymer whose segments differ in surface energy ($\gamma_{PDMS} = 15-24 \times 10^{-3}$ N/m, $\gamma_{PI} = 37-41 \times 10^{-3}$ N/m) (20), block segments having lower surface energy will orient toward the surface (21). Very high surface concentrations of PDMS (∼90%) have been observed in bulk copolymers having as little as 1% PDMS content (21−26). Subsequently, the PDMS near the surface is transformed at least partially to SiO_2 by high irradiation levels and/or AO. Thus, such systems provide a significant degree of protection. Siloxane containing block- and graft-copolymers have been successfully tested either in oxygen plasma or even in the real space environment and show excellent passivation tendencies (3, 16, 27−31).

Weight loss measurements following AO exposure have shown that siloxane can protect polymer systems from aggressive AO, and a significant degree of protection (decrease in weight loss by 80−98%) has been observed (27). Compared with SiOx coated PI samples, the PI-*b*-PDMS systems have also shown an improvement in durability to AO after exposure to VUV or thermal cycling combined with VUV exposure. For 10−20 wt % PDMS concentrations, the modified films showed nearly identical initial moduli compared to the unmodified PI, but an increase in toughness was observed. However, the changes in solar absorption are still a problem.

In this study, commercially available amino-terminated polysiloxanes with different molecular weights are used for the synthesis of PI-*b*-PDMS block copolymers. This extends the study of Bott et al. (28, 32, 33) in order to perform a structural optimization with respect to maximum protection. A variation of the PDMS block length will enable control of the level of surface enrichment and the block length of the PI controls the gradient of surface composition. In addition to the usual multi-block structure $-[-\text{PDMS-}b\text{-PI}-]_n-$ (Figure 1), we have synthesized tri-block copolymers PDMS-*b*-PI-*b*-PDM using mono-amino-terminated PDMS as well as star-shaped and branched structures using a trifunctional amine component. The state of the art is advanced by improving the control of the chemistry of copolymer formation, resulting in a better control of phase separation even at small loads. This influences the in situ formation and repair of the protective layer.

MATERIALS AND PROCEDURES

The following monomeric components were used for the synthesis (Scheme 1).

These monomers offer a wide variety of different compositions. They also allow the formation of multiblock copolymers when using the difunctional amino-terminated siloxanes and triblockcopolymers when using monofunctional amino-terminated PDMS (Scheme 1). Additional starlike structures and branched structures can be realized using the trifunctional amines. The PDMS components, Fluid NH15D, Fluid NH40D, Fluid NH130D, SLM446011-65, and SLM446011-15 have been supplied by Wacker Silicones. The average molecular weight of the PDMS part in the diamino end-capped silicones of the NH series was 1350, 3050, and 11000 g/mol for NH 15D, NH 40 D, and NH 130 D, respectively, and for the monoamino end-capped silicones SLM446011-65 and SLM446011-15, 4600 and 1100 g/mol, respectively. Pyromellitic dianhydride 97% (PMDA), 3,3′,4,4′- biphenyl tetra carboxylic dianhydride 97% (BPDA), *N*-methyl-2-pyrrolidon (NMP) anhydrous >99,5%, and tetrahydrofuran (THF) anhydrous >99.9% were purchased from Aldrich and 4,4′ oxidianiline 98% (ODA) from Fluka. All materials are used as received from the supplier. The water content of the reactants was controlled by NMR. It is important to use inhibitor-free solvents (THF and NMP) for the polymer synthesis

Scheme 1. Structures of the Used Monomers

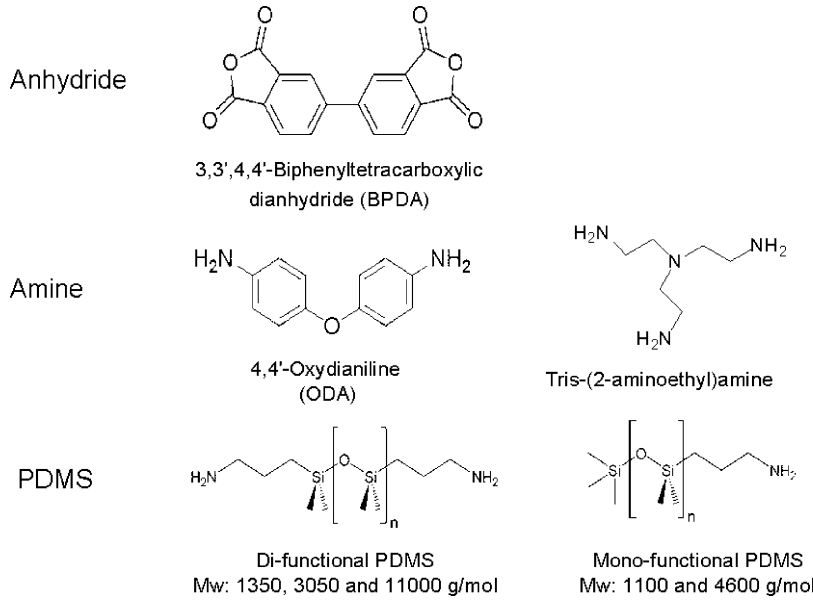

to enable sufficiently high molecular mass and by that to enable sufficient mechanical strength of the final films.

The polymers were synthesized according to the following procedure with a PDMS content varying between 0 and 41 wt %. First, the precursor for the poly(imide) blocks, the poly amide-acid has been prepared. A solution of the aromatic amine component ODA reacts at 25 °C with the solid dianhydride (BPDA), added under stirring the solution. Consequently, an excess of dianhydride was added in case of mixed amine components and anhydride terminated chains (imide blocks) will be formed in a first step. Subsequently, the remaining amine part (PDMS derivatives) was added to the reaction mixture, leading to the formation of the final multiblock structure when using diamino-terminated PDMS or triblock structure when using monoamino-terminated PDMS. For the synthesis, a mixture of NMP and THF is used as a solvent, and the synthesis is carried out under dry nitrogen as a protective gas.

Alternatively, the mostly described synthetic procedure (25, 32−34) starts with a reaction of the diaminsiloxanes with the dianhydride, to form anhydride-terminated siloxane blocks followed by an addition of the remaining monomers to form the multiblock copolymer. Although this method should result in possibly a better defined system having less haziness because of phase separation of different parts caused by the different solubility of the polymide and the PDMS, the resulting polymers and films were not different from those obtained by the earlier described method.

The obtained polymer solutions are centrifuged to remove particles prior to film casting on glass substrates, performed in a clean room using a casting knife (750 μm slit). The solvent was subsequently evaporated in a flow-box with an anhydrous nitrogen flow at room temperature until the film was tack-free. The films were finally imidized in steps of one hour at 150, 250 and at 350 °C. Additionally to the in this study synthesized polymers and prepared films, an industrial sample of a polyimide PDMS block copolymer film (SBA-A-030) as provided by Nippon Steel Incorp. has been included in the characterization program. This film is equivalent to the BSF 30 sample described in an earlier study (30, 31).

Testing. The films were characterized with respect to their mechanical, thermal and surface properties, optical appearance and for their performance in simulated on-ground and LEO environment (exposure to AO, thermal cycling and humidity). The investigated properties include contact angle, surface roughness, AO weight loss, solar absorptance, tensile testing, and electrical conductivity.

Mechanical and Thermal Characterization. The mechanical characterization was performed by tensile testing of strips of the films with a crosshead speed of 5 mm/min at ambient temperature. Further thermal and mechanical characterization was performed by differential scanning calorimetry (DSC) and thermo-gravimetric analysis (TGA) (rate 10 K/min) as well as by dynamic-mechanical thermal analysis DMTA at 3 different frequencies (0.1, 1, and 10 Hz) with a rate of 2.5 K/min; all methods were operated under N_2.

Electrical Characterization. The volume resistivity was measured according ASTM D-275 using a Keithley 6517A electrometer in combination with a Keithley 8009 test fixture operating at 200 pA at 500 V DC.

Outgassing and Atomic Oxygen Test. Previous to the AO test, an outgassing test at 125 °C and at a pressure $<1 \times 10^{-5}$ mbar was performed for 24 h. AO exposure studies using the ESTEC ATOX facility was performed afterward. This simulator consists of a vessel composed of three compartments separated by two electro-pneumatic valves: the nozzle compartment where the breakdown is produced, the main chamber and the sample compartment. The vacuum in main chamber during AO exposure is below 2×10^{-4} mbar. The system layout is shown in Figure 3. The source concept is based on the Laser Pulse Induced Breakdown (LPIB) principle, first, molecular oxygen is forced through the throat of a nozzle, in the form of gas puffs generated by a fast-switching molecular beam valve. After partial fill of the nozzle, a high power beam from a pulsed CO_2 laser (wavelength 10.6 μm) synchronized with the valve is focused onto the injected gas. This produces breakdown and dissociation of the gas into a very hot (>20 000 K) plasma. The detonation creates a blast wave that propagates through the nozzle with, as well-known from the theory of gas dynamics, conversion of the plasma thermal energy into directed velocity. The cooling of the expansion allows the plasma to charge neutralize into oxygen atoms, but the expansion rate is kept sufficiently high, and the density sufficiently low, to prevent recombination of these atoms into molecules. A thermally cold (low spread in random velocity - meaning a couple of thousand Kelvin) AO beam with high directed energy finally exhausts the nozzle and propagates toward the samples. The AO velocity is obtained measuring the time-of-flight by recording with a memory oscilloscope the signals provided by two photomulti-

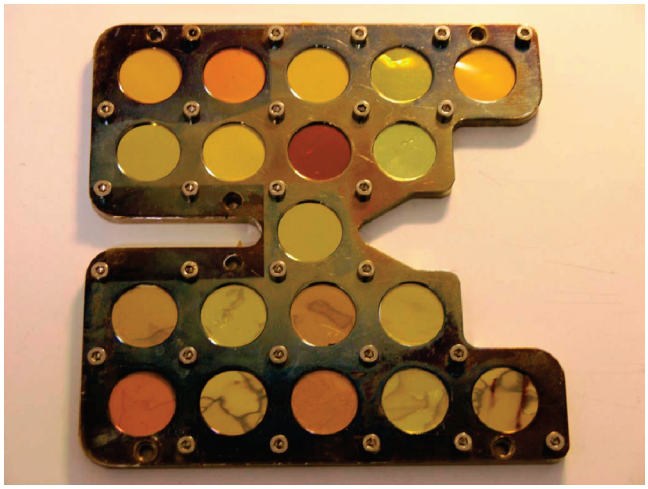

FIGURE 2. Samples mounted in AO exposure tray, with circular mask overlaid (three films are the Kapton reference samples).

pliers and is on average 7.5 ± 0.5 km/s and the angle of AO attack is 0°. The AO flux is measured by the mass loss of Kapton HN reference samples; the AO fluence for the first test 1 was 2.8×10^{20} atoms/cm^2. A second test was performed on samples with higher contents on PDMS using three exposures with fluencies of 2.5×10^{20}, 1.5×10^{20}, and 3.11×10^{20} Atoms/cm^2. This gives a total fluence of 7.11×10^{20} atoms/cm^2. In the standard setup, 19 samples (20 mm ×20 mm square) are integrated into the sample holder. The samples were mounted in the standard AO exposure tray, such that each sample was covered by a circular mask, and the central irradiated area had a diameter of 15 mm. The setup at the beginning of the exposure is shown in Figure 2.

The sample analysis consisted of visual inspection, mass measurement, thermo-optical, and transmission as well as reflection measurements in the wavelength range of 200−2500 nm.

Thermal Cycling and Temperature−Humidity Test. The thermal cycling (T/C) test consisted of 50 cycles between −100 °C and +100 °C and 50 cycles between −150 °C and +150 °C (heat-up/cool-down 60 K/minute, no dwell) and the temperature−humidity (T/H) test was performed for 8 days exposure at 35 °C and 85% RH. Subsequently to both tests, the samples were inspected visually and checked with respect to possible dimensional and weight changes.

Morphological and Surface Characterization. Besides an inspection of the samples before and after AO exposure by optical microscopy, detailed analysis of the roughness of the films has been analyzed via confocal microscopy (Sensofar) and atomic force microscopy in contact and noncontact mode. Contact angles of water droplets on the pristine and exposed film surfaces as an indication of the surface composition were determined using a Kruess DSA 100 apparatus.

RESULTS AND DISCUSSION

The synthesis of the polymers was performed according to a composition matrix approach varying the length, amount and functionality of the PDMS monomers in a systematic way with the aim to indicate the most promising architectures. The polycondensation reaction proceeds instantaneously after addition of the anhydride BPDA onto the amine solution, as indicated by a change in color from colorless to yellow. Already after an hour a strong increase in viscosity is observable. The samples containing PDMS are hazy since the siloxane-amine monomers are not miscible with NMP. Consequently, the resulting casted and cured films are also not transparent but hazy like observed earlier by Jwo et al. (35) In generally, smaller chains of PDMS (NH 15 D) are better compatible than longer chains (NH 130 D), and monofunctional PDMS derivatives (SLM 446011) are less compatible with the final polymide blocks and hence are less soluble. Compatibility problems start consequently already at concentrations as low as 6% in the case of NH 130 D and also of SLM 446011-65. To still maintain a homogeneous system, we have increased the amount of cosolvent THF in cases of higher concentration on PDMS containing monomers and high-molecular-weight PDMS monomers like NH40D and NH130D as well as SLM446011-65. The cured yellow and transparent films are smooth, strong, and flexible with a thickness between 30 and 50 μm (see Figure 3). A complete table of the synthesized polymers and the properties of the polymeric films can be found in the Supporting Information section.

All films with shorter PDMS blocks appear somewhat darker in color; the block copolymers with contents higher than 25 wt % are translucent and not completely transparent. The use of higher concentrations (>10% PDMS) of monoamino-terminated PDMS derivatives is limited because of the stoichiometry the length of the resulting polymer chains, leading to brittle films. This obstacle has been overcome by the addition of a small amount (1% of the aromatic amine ODA) of trifunctional monomer (tris(2-aminoethyl)amine), which consequently leads to branched and starlike architectures with a higher molecular weight than strictly linear polymers and thus preventing the films from being brittle.

The thermogravimetric analysis shows that all films appear to absorb a small amount of moisture (0.1%), which is evident from the initial weight loss between 25 and 100 °C. Under dynamic conditions, i.e., using a heating rate of 10 K

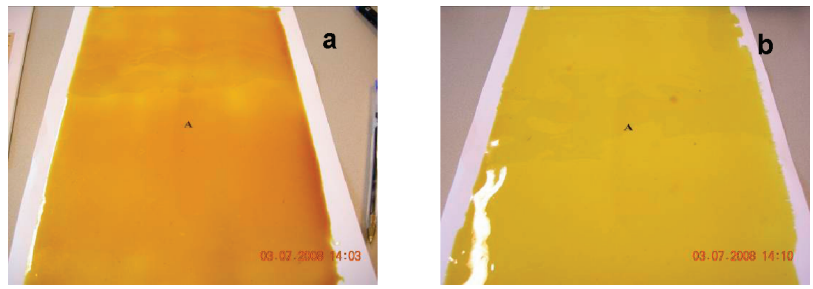

FIGURE 3. Pictures of casted films poly (siloxane imide) block copolymers using the difunctional PDMS NH 40D containing: (a) 2 wt % and (b) 6 wt % PDMS in the final composition. The films are very smooth, homogeneous, and transparent.

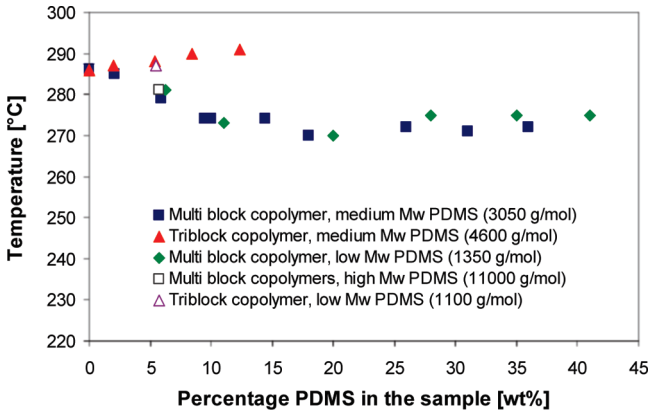

FIGURE 4. Glass transition temperature vs PDMS content for the PI-PDMS block copolymers with different architectures.

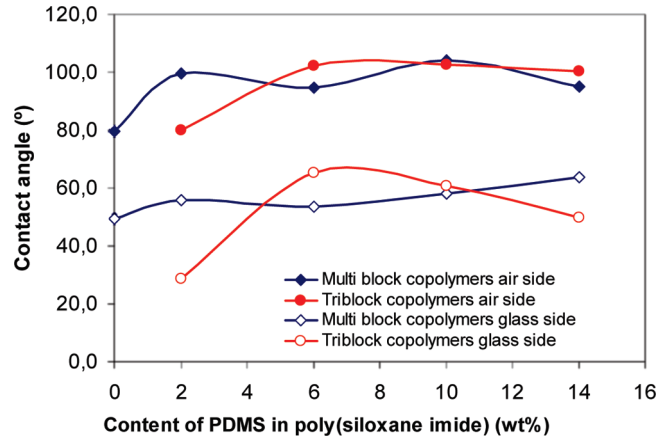

FIGURE 5. Contact angle vs PDMS content for PI-PDMS block copolymers.

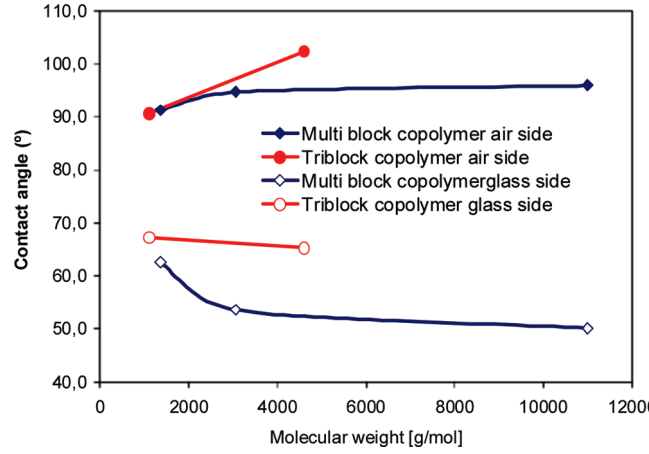

FIGURE 6. Contact angle of di- and monofunctional PDMS in Poly (siloxane imide) against molecular weight of PDMS. All samples contain the same load (6%) of PDMS.

min^{-1}, the films show excellent thermal stabilities and the obtained values are similar to that of all-aromatic polyetherimide s (39). The calorimetrical experiments show no discernible transitions, i.e., crystallization, melting, or T_g in the temperature range up to 400 °C. All films good mechanical properties at room temperature (moduli 2−7 GPa) as well as at elevated temperatures (200 °C: 1−4 GPa). This result is not at all surprising because the synthesis was carefully controlled and optimized to achieve high molecular weights, which ensure good mechanical properties. The surprisingly high glass-transition temperatures as determined by DMTA also for compositions with high contents of PDMS qualify these materials for an application in space and confirm and extend earlier reported data (28, 32, 33) (see Figure 4).

All films are tough, with a tensile strength between 50 and 150 MPa and an elongation at break between 4 and 15%. The mechanical behavior is very similar to the behavior of all-aromatic polyetherimides (39) and again suitable for an application in LEO. The industrial sample SBA-A-030 shows a substantial decrease in the mechanical properties already starting at 100 °C, the T_g at 150 °C is too low for an application of this material in space.

The spontaneous enrichment of Si-containing molecules and parts of polymeric chains in case of copolymers has been shown earlier in an impressive manner by several different groups. This behavior is also observable for PDMS containing multiblock copolymers; here it has been previously demonstrated, that already small loads of Si-containing monomers in the polymer composition as well as segments of the length of 4 monomeric units show a almost complete surface coverage (24, 25).

Similar results have been found in this study; here already with a load of 2% PDMS (in case of the multiblock copolymers), a complete surface coverage of the PDMS has been found (Figure 5).

The contact angle, as determined on the air-facing side of the casted films, increases quickly to values known for PDMS-homopolymer surfaces. It is noticed that the increase in the contact angle occurred for the multiblock copolymers using difunctional PDMS macromers already at concentrations of 2 wt %, just like that observed in earlier studies (26, 36−38), whereas for the triblock-copolymers using the monofunctional PDMS compounds, the contact-angle increase occurred at a concentration of about 6 wt % siloxane. The difference in the threshold of content of PDMS for a complete surface coverage of the PDMS blocks between multiblock copolymers and triblock copolymers has been observed first in this study and may be coupled to an insufficient surface coverage of the siloxane blocks in case of triblock copolymers with low content of PDMS. The contact angle on the glass-facing side of the casted films remains nearly constant and displays much lower values corresponding to the polyimide fraction of the block copolymers. Therefore, the spontaneous surface enrichment of the siloxane blocks can be demonstrated.

Interesting also is a comparison of the effect of surface enrichment of PDMS as expressed by the contact angle of the air surface of the casted films in contact with water for the same load on PDMS (6 wt %) for different molecular weight PDMS derivatives (see Figure 6).

The triblock-copolymers offer a higher mobility to the PDMS blocks because they are attached at the periphery of each macromolecule and consequently higher contact angles (better separation) are observable for the monoamino-terminated PDMS derivatives containing materials. On the

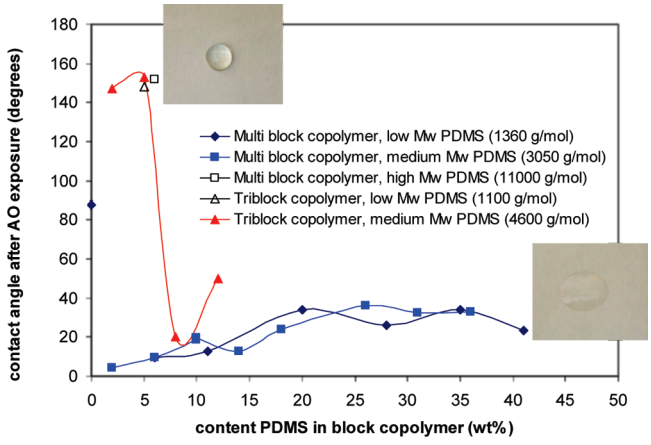

FIGURE 7. Contact angle vs PDMS content for PI-*b*-PDMS block copolymers after AO exposure. The insert are photographs of a water droplet on the block copolymer surface before and after AO exposure showing a drastic decrease in contact angle due to the formation of a silica layer on the irradiated surface.

other side, obviously a minimum amount of PDMS blocks is needed for complete surface coverage, as seen in Figure 5.

The thermal cycling and the temperature/humidity test showed no significant changes in the performance of all samples within the nominal range and the test accuracy; from this perspective, the films can be classified as being suitable for LEO. Previous to the AO exposure, an outgassing test according to ECSS Q-ST-70-02 was performed in order to determine the possible danger on contamination of cold parts in space by heating to 125 °C for 24 h in a vacuum. All synthesized samples showed a total mass loss (TML) lower than 1 % with a volatile condensable material (VCM) of a maximum of 0.16 %. In contrast, the industrial sample SBA-A-030 performed much different, here a TML of 3.9 % and a VCM of 3.7 % were determined, which fails the nominal screening test requirements for space. Massive outgassing will lead to contamination of sensitive systems and areas.

The surface-enriched PDMS layer is subsequently transferred under action of AO (and UV) into SiO_2,. The transformation of a PDMS surface into a thin layer of SiO_2 is already well-known and has also been shown for such block copolymers (30, 31, 34). Such a transfer is, for example, manifested in a change in surface morphology but also in a drop in contact angle displayed by the surfaces in contact with water, because silica is hydrophilic and hence attracts water. Indeed, the predicted drop in contact angle is observable (see Figure 7); however, it is mainly in the case of the samples with the multiblock morphology and then only for the samples using small and medium difunctional PDMS macromers.

Again, the triblock copolymer samples show rather high contact angles, in contrast to the expected small contact angles, because of the formation of a surface SiO_2. The reason for this is yet unclear and will be further investigated. The transfer of the surface-enriched PDMS layer into a thin silica layer should finally result in a decrease in AO erosion rate of the material because the formed silica layer should

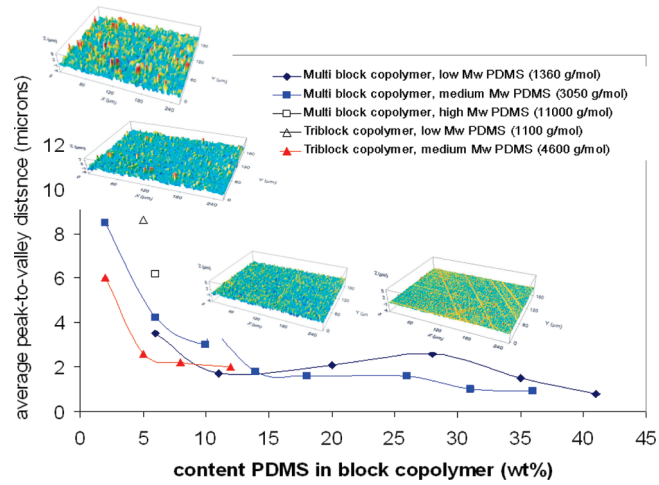

FIGURE 8. Plot of the average peak-to-valley distance of the surface structures obtained after AO exposure as measured by confocal microscopy of the block copolymer films for different architectures vs PDMS content for PI-PDMS block copolymers. The insert are 3D pictures of the confocal microscopically inspection of samples with different PDMS contents.

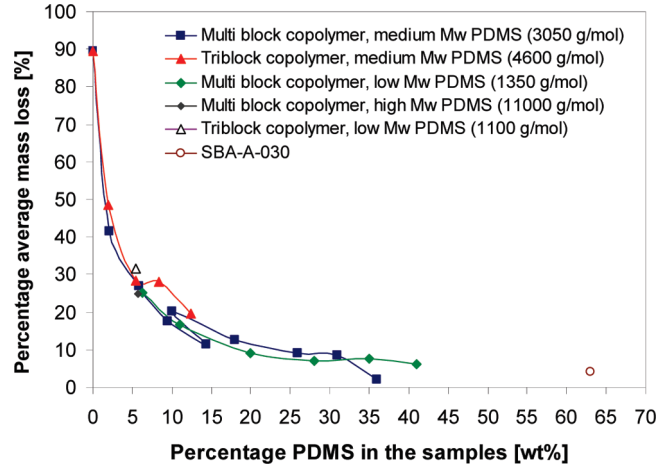

FIGURE 9. Plot of the average mass loss of the polyimide-PDMS block copolymers related to the Kapton reference samples.

protect the underlying material from oxygen-initiated erosion, resulting in a drastic decrease in surface roughness observable after AO exposure already for small loads like 6 wt % PDMS (see Figure 8).

The surface of the eroded films containing 6 wt % PDMS and more in the block copolymer composition is rather smooth and an inspection by SEM shows the formation of a dense surface layer of silica due to AO exposure. The formation of a smooth protective silica surface is also manifested by a decrease in mass loss compared to the Kapton reference samples similar to earlier studies (27, 28, 30–33). Again, already small loads of PDMS show a substantial effect, the AO erosion rate can be reduced to 10 % of the comparative rate observed for Kapton for loads of PDMS starting at about 14 wt % (see Figure 9).

In Figure 10, the amount of PDMS is plotted versus the loss of mass after the first, the second and the third exposure as explored in detail in the second set of AO exposure experiments. The various types of PDMS do not seem to

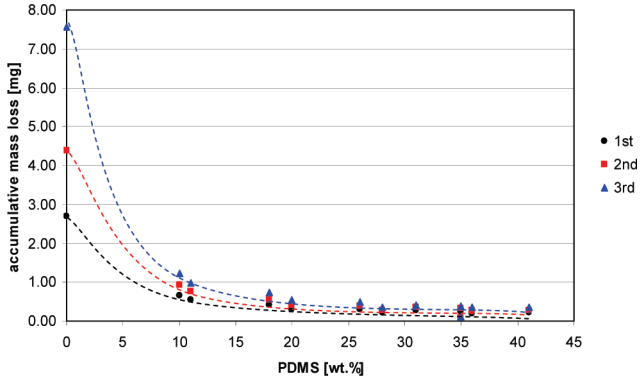

FIGURE 10. Plot of the accumulative average mass loss related to the Kapton reference samples for multiblock copolymers with small and medium molecular weight PDMS blocks showing a leveling off of the mass loss for different consecutively exposure experiments (1st with 2.5 × 10^{20} atoms/cm^2, 2nd with 1.5 × 10^{20} atoms/cm^2, and the 3rd with 3.11 × 10^{20} atoms/cm^2) starting at a content of PDMS in the block copolymers of about 15 wt %.

differ much from each other. It can be seen that the amount is the crucial factor that inhibits AO erosion.

The silica surface formed by reaction with AO acts as intended and protects the underlying matrix polymer from further AO-related erosion process. The results obtained are in line with results of comparable experiments in the literature and with other techniques of PI surface protection like Photosil, Implantox, etc.

The thermo-optical measurements of the films after AO exposure shows only a slight increase in absorption as well as in infrared emissivity to a certain extent (α, 0.37 + 0.02; ε, 0.82 + 0.02; compared to Kapton α, 0.32 + 0.1; ε, 0.72 − 0.025) and seems to become constant after some time or fluence, respectively. This is different for the aromatic polyimide sample; here, a stronger increase in absorption and a decrease in emissivity versus exposure duration is observable. Two effects may influence the transmission: the roughening of the surface results in an increased scattering of the incoming light and therefore in a reduced transmission; and a possible thinning of the sample would increase the transmission. The second effect is clearly less dominant for the block copolymers. The environmental tests demonstrate that the samples survive typical satellite temperature−humidity and thermal cycling tests. The determined volume resistivity values range from 1 to 5 × 10−16 Ω cm, which is comparable to the volume resistivity of Kapton reference material and does not change significantly (<factor 2) after the thermal cycling test. A decrease in the volume resistivity values by factors up to 10 during temperature−humidity test has been determined. However, the values are restored to pretest values within 1−2 days after the test. Altogether, the environmental tests show no differences in the performance of the films tested and as such no dependency of the performance on the length and amount of the PDMS blocks in the block copolymers.

CONCLUSIONS AND OUTLOOK

The synthesized block copolymers show in general interesting and sufficient thermo-mechanical and electrical properties as well as AO resistance to qualify them or use as, for example, thermal blanket material in space. Upon AO exposure, as a consequence of the oxidation of the block copolymer and especially of the surface-enhanced PDMS layer, a thin SiO_2 film has been formed. This layer protects the polymeric material underneath from further degradation. Triblock copolymers appear to be less suited for the envisaged application, because they display more difficulties with respect to processing or to generate a clear homogeneous film for the loads on PDMS required for the formation of a close glass surface. Multiblock copolymers starting with 12 wt % PDMS show only a small weight loss of about 10−15% after AO exposure compared to Kapton and display a fairly smooth surface and are thus better suited. Also the neglectable outgassing with a determined TML < 1 % and VCM ≈ 0.05% meets the screening test specifications for use in space. The only film with no visible mark after exposure is a commercial sample from Nippon Steel. However, this sample, which also contains a very high amount of PDMS, displays a rather low T_g and a high mass loss in vacuum and is hence not suitable for space applications.

Because polysiloxane-*block*-polyimide film has a thin, flexible, hard, and robust surface coating for AO protection, it is easy to handle during spacecraft manufacturing. Such polysiloxane-*block*-polyimides have a high potential to provide many advantages as a space-use material and can especially improve reliability, design flexibility, and cost effectiveness for LEO spacecrafts. The produced materials show damaged self-healing of the protective surfaces upon further AO irradiation as expected in a LEO environment (31).

Acknowledgment. This work was performed within the in the framework of ESTEC in an Innovation Triangle Initiative (ITI) Project #21229/07/NL/CB. The supply of the amino-functionalized PDMS oligomers by Wacker Silicones is gratefully acknowledged.

Supporting Information Available: Additional tables (PDF). This material is available free of charge via the Internet at http://pubs.acs.org.

REFERENCES AND NOTES

(1) Raja Reddy, M. *J. Mater. Sci.* **1995**, *30*, 281.
(2) Dever, J. A.; Bruckner, E. J.; Rodriguez, E. *Synergistic Effects of Ultraviolet Radiation, Thermal Cycling, and Atomic Oxygen on Altered and Coated Kapton Surfaces*; NASA Technical Memo 105363/Report AIAA-92-0794; National Aeronautics and Space Administration: Washington, D.C., 1992.
(3) Schwam, D.; Litt, M. H. *Adv. Perform. Mater.* **1995**, *3*, 153.
(4) H. Shimamura, H. T.; Nakamura, T. *Polym. Degrad. Stab.* **2009**, *94*, 1389.
(5) Banks, B. A.; Snyder, A.; Miller, S. K.; Demko, R. *Issues and Consequences of Atomic Oxygen Undercutting of Protected Polymers in Low Earth Orbit*; NASA Technical Memo 2002-211577; National Aeronautics and Space Administration: Washington, D.C., 2002.
(6) Banks, B. A.; Snyder, A; Miller, S. K.; de Groh, K. *J. Space. Rock* **2004**, *41*, 335.
(7) Tennyson, R. C. *High Perform. Polym.* **1999**, *11*, 157.
(8) Gudimenko, Y.; Ng, R.; Kleiman, J.; Iskanderova, Z.; Milligan, D.; Tennyson, R. C.; Hughes, P. C. *J. Spacecr. Rockets* **2004**, *41*, 326.
(9) Iskanderova, Z.; Kleiman, J.; Gudimenko, Y.; Tennyson, R. C.; Morison, W. D. *Surf. Coat. Technol.* **2000**, *127*, 18.

(10) Tan, H.; Ueda, M.; Dallaqua, R.; Rossi, J. O.; Beloto, A. F.; Demarquette, N. R.; Gengembre, L. *Jpn. J. Appl. Phys.* **2005**, *44*, 5211.
(11) Iskanderova, Z. A.; Kleiman, J.; Morison, W. D.; Tennyson, R. C. *Mater. Chem. Phys.* **1998**, *54*, 91.
(12) Kleinman, J. *MRS Symp. Proc.* **2005**, *851*, NN8.6.1.
(13) Matienzo, L. J.; Egitto, F. D. *J. Mater. Sci.* **2006**, *41*, 6374.
(14) Dworak, D. P.; Soucek, M. D. *Prog. Org. Coat.* **2003**, *47*, 448.
(15) Dworak, P. D.; Banks, B. A.; Karniotis, C. A.; Soucek, M. D. *J. Space. Rock.* **2006**, *43*, 393.
(16) Duo, S.; Li, M.; Zhua, M.; Zhoua, Y. *Mater. Chem. Phys.* **2008**, *112*, 1093.
(17) Graubner, V.-M.; Jordan, R.; Nuyken, O.; Schnyder, B.; Lippert, T.; Koltz, R.; Wokaun, A. *Macromolecules* **2004**, *37*, 5936.
(18) Kuckertz, V. H. *Makromol. Chem.* **1966**, *98*, 101.
(19) Maudgal, S.; St Clair, T. L. *Int. J. Adhes.* **1984**, *4*, 87.
(20) Brandrup, J, Immergut, E. H., Grulke, E. A., Eds. *Polymer Handbook*, 4th ed.; John Wiley and Sons: NewYork
(21) Li, L.; Chan, C.-M.; Liu, S.; An, L.; Ng, K.-M.; Weng, L.-T.; Ho, K.-C. *Macromolecules* **2000**, *33*, 8002.
(22) Gilman, J. W.; Schlitzer, D. S.; Lichtenhan, J. D. *J. Appl. Polym. Sci.* **1996**, *60*, 591.
(23) McGrath, J. E.; Dunson, D. L.; Mecham, S. J.; Hedrick, J. L. *Adv. Polym. Sci.* **1999**, *140*, 61.
(24) Zhao, J.; Rojstaczer, S. R.; Chen, J.; Xu, M.; Gardella, J. A., Jr. *Macromolecules* **1999**, *32*, 455.
(25) Mahoney, C. M.; Gardella, J. A., Jr.; Rosenfeld, J. C. *Macromol* **2002**, *35*, 5256.
(26) Furukawa, N.; Tamada, Y.; Furukawa, M.; Yuasa, M.; Kimura, Y. *J. Polym. Sci., Part A: Polym. Chem.* **1997**, *35*, 2239.
(27) Rutledge, S. K.; Cooper, J. M.; Olle, R. M. *The Effect of Atomic Oxygen on Polysiloxane-Polyimide for Spacecraft Applications in Low Earth Orbit*; NASA Technical Memo AIAA-91-20735; National Aeronautics and Space Administration: Washington, D.C., 1991.
(28) Bott, R. H.; Summers, J. D.; Arnold, C. A.; Taylor, L. T.; Ward, T. C.; McGrath, J. E. *J. Adhes.* **1987**, *23*, 67–82.
(29) Dworak, D. P.; Soucek, M. D. *Prog. Org. Coat.* **2003**, *47*, 448.
(30) Yokota, K.; Abe, S.; Tagawa, M.; Iwata, M.; Miyazaki, E.; Ishizawa, J.-I.; Kimoto, Y.; Yokota, R. *High Perform. Polym.* **2010**, *22*, 237.
(31) Miyazaki, E.; Tagawa, M.; Yokota, K.; Yokota, R.; Kimoto, Y.; Ishizawa, J. *Acta Astron.* **2010**, *66*, 922.
(32) Arnold, C. A.; Summers, J. D.; Chen, Y. P.; Bott, R. H.; Chen, D.; McGrath, J. E. *Polymer* **1989**, *30*, 986.
(33) Arnold, C. A.; Summers, J. D.; McGrath, J. E. *Polym. Eng. Sci.* **1989**, *29*, 1413.
(34) Park, H. B.; Han, D. W.; Lee, Y. M. *Chem. Mater.* **2003**, *15*, 2346.
(35) Jwo, S.-L.; Whang, W.-T.; Liaw, W.-C. *J. Appl. Polym. Sci.* **1999**, *74*, 2832.
(36) Cho, C. K.; Kang, J. H.; An, Y. T.; Cho, K.; Park, C. E.; Huh, W. *J. Adhes. Sci. Technol.* **2000**, *14*, 107.
(37) Rimdusit, S.; Benjapan, W.; Assabumrungrat, S.; Takeichi, T.; Yokota, R. *Polym. Eng. Sci.* **2007**, *47*, 489.
(38) Sysel, P.; Hynek, V.; Sipek, M. *Collect. Czech. Chem. Commun.* **1998**, *63*, 53.
(39) Stienstra, M. M.; Dingemans, T.; Van Eesbeek, M.; Rohr, T. *High Perform. Polym.* **2008**, *20*, 461.

AM100223V